INTERNATIONAL JOURNAL FOR NUMERICAL METHODS IN FLUIDS, VOL. 3, 347–361 (1983)

# NUMERICAL SIMULATION OF LIQUEFIED FUEL SPILLS: II. INSTANTANEOUS AND CONTINUOUS LNG SPILLS ON AN UNCONFINED WATER SURFACE

JULIUS BRANDEIS AND DONALD L. ERMAK

*Lawrence Livermore National Laboratory, P.O. Box 808, L-451*
*Livermore, California 94550, U.S.A.*

## SUMMARY

A simple numerical model based on the shallow water equations in radial symmetry is used to simulate both instantaneous and continuous spills of liquefied natural gas (LNG) onto a water surface. Using the computed results, a study is made of the similarities and differences in the pool structure resulting from the two types of spills. For instantaneous spills a relation linear on a logarithmic plot is suggested between the maximum pool size and the spill volume. The effects of shear forces and surface cohesivity on the evolution of the spill are also examined.

KEY WORDS Shallow Water Equations LNG Pool Spreading Continuous and Instantaneous Spills

## INTRODUCTION

In this, the second of two papers dealing with modelling of spills of liquefied fuels, attention is turned to the specific problem of the discharge of LNG onto a water surface. The numerical model described in the first paper[1] is used to study unconfined spills such as those potentially resulting from a break-up of an LNG carrier. The largest of these ships can carry up to 125,000 $m^3$ of the fuel in five compartments, damage to any one of which could result in a release of 25,000 $m^3$ of liquefied gas at a rate dependent on the extent of the damage. There exist a number of simple, algebraic models[2–4] capable of predicting approximately the maximum size and duration of the spread of the liquid released from such spills. These are not, however, sufficient for modelling the detailed dynamics of the spill. The knowledge of such details is essential to the numerical simulation of the dispersion of the gas evaporated from the pool. Modelling of heavy gas dispersion using three-dimensional finite difference and finite element approaches is an ongoing programme at LLNL. The present method has been used to supply the time-history of the evaporation source for these gas dispersion codes, which were used for simulating the LNG spill experiments carried out at China Lake.[5]

Both continuous and instantaneous spills of LNG will be considered in this paper. For the present purpose, the term continuous will always refer to those spills in which LNG is added at the source at a constant rate and for a finite time duration. The instantaneous spills will always be understood to refer to the collapse of an initial LNG volume of arbitrary shape onto the water surface. In both cases, the LNG is assumed to be submerged to a depth determined by the buoyant equilibrium with the water.

It will be shown that the present numerical model, despite its simplicity, is capable of

0271–2091/83/040347–15$01.50

*Received 4 February 1982*
*Revised 12 July 1982*

reproducing the essential features of the spreading liquid observed experimentally, and is in good agreement with available data. Using the model, a detailed comparision is presented of the continuous and instantaneous spills. It confirms the basic conclusions of Raj[6] but goes into considerably more detail in examining the subject of the structure and evolution of such spills.

Until now it has been tacitly assumed in the discussion that the fluid is inviscid and that the surface tension effects may be ignored. Though this was sufficient for the above mentioned purposes, it is, strictly speaking not correct. Fay[7] identifies and defines the three stages in the evolution of the spill, categorized on the basis of the dominant forces acting in each phase. These are: gravity-inertia, gravity–viscous and surface tension–viscous. An effort will be made here to present models for the friction and surface tension effects and to examine the influence of these factors on the evolution of the spill. Formulation of the viscous term is a non-trivial matter for reasons to be described later. Two different viscosity models are considered in this work, and their effectiveness will be described later. The surface tension effect becomes important only during the last phase of the spill. It is this effect that determines the minimum value for the thickness of LNG.[8] After this thickness is reached, the thin LNG layer breaks up into droplets since the surface tension is no longer capable of keeping the layer continuous. A simple approach to modelling this phenomenon, based on empirical information will be proposed.

## FORMULATION

The mathematical model used in this study consists of depth-averaged, shallow water equations modified for mass addition and evaporation. Conservation of mass is expressed in terms of the liquid pool height equation. It is derived for an incremental cylindrical volume of the radially spreading pool and is given by

$$\frac{\partial(rh)}{\partial t}+\frac{\partial(urh)}{\partial r}+(v-w)r=0 \tag{1}$$

where $h=h(r, t)$ is the height of the LNG pool at radius $r$ and time $t$, $u=u(r, t)$ is the local horizontal velocity, and $w$ is the liquid fuel source rate expressed as a velocity. The liquid fuel is assumed to evaporate from the pool with a constant velocity $v$.

The momentum equation is

$$\frac{\partial u}{\partial t}+\frac{\partial}{\partial r}\left(\frac{u^2}{2}+\delta g h\right)+\frac{\tau}{\rho h}+\frac{w}{h}u=0 \tag{2}$$

where $g$ is the acceleration of gravity, $\delta=1-\rho/\rho_s$, $\rho$ is the density of the spilled liquid (LNG), $\rho_s$ is the density of the surface liquid (water) and $\tau$ is the shear force at the fuel–water interface (models for $\tau$ will be described in a later section). Incorporated in equation (2) is the relationship for average hydrostatic pressure, given by

$$P=\tfrac{1}{2}\rho g h \tag{3}$$

In the continuous spill mode, liquid fuel is continually injected into the pool at a constant velocity, $w$. The mass flow rate is then given by $\pi\rho w R_0$, where $R_0$ is the source radius. Following the spill shut-off, $w=0$.

In the instantaneous spill mode an initial fuel volume is specified and $w$ is set equal to zero. This initial fuel volume is assumed to have a parabolic cross-sectional shape with any desired ratio of height to radius and is at the equilibrium depth specified by the density of the

two liquids. (Other shapes of the initial volume are admissible by the model. Parabolic was felt to be more realistic than the rectangular shape which might more closely model the truly instantaneous spill.)

The boundary conditions needed to complete the formulation are

$$u = 0 \quad \text{at} \quad r = 0 \tag{4}$$

$$u = 0 \quad \text{at} \quad r > r_{LE} \tag{5}$$

where $r_{LE}$ is the instantaneous location of the leading edge of the pool defined as the value of $r$ for which $h = 0$. The value for $h$ at $r = 0$ is found from the appropriate compatibility condition.[1]

Equations (1) and (2), subject to the conditions given by equation (4) and (5) are solved using the method described in Reference 1.

## CONTINUOUS VS. INSTANTANEOUS SPILLS

An instantaneous spill is the limiting case of a finite volume, continuous spill with an infinite spill rate. Such an ideally instantaneous spill is unlikely to occur, but does represent a conceptual limiting case. A continuous release of LNG from a ruptured tank is more likely. It is of considerable interest, therefore, to examine both categories of spills, using the numerical model described in this paper. The spreading characteristics of the two spill categories are of particular interest, since they determine the rate of formation of the volatile, heavy gas cloud.

Figure 1 presents a sketch of the radial cross-section of typical continuous and instantaneous spills conducted on a water surface, as computed by the present numerical model. The fluid, for the time being, is idealized as inviscid and the surface tension is ignored. The instantaneous spill quickly forms a shock front at the leading edge, which propagates outward. (This subject is treated in more detail in Reference 1.) After a short time, the material at the centre of the pool becomes very thin and disappears by evaporation. Thus, the spreading liquid pool takes on an annular shape (experimentally confirmed in Reference 9), with both the inner and the outer boundaries moving outward until all the material evaporates.

By contrast, in the continuous spill the material is continuously added at the source for the duration of the spill. The liquid spreads outward (forming a weak leading edge shock), eventually (providing that sufficient volume was released) reaching a critical surface area for which an equilibrium exists between mass added and mass evaporated out of the pool. The pool is then said to be in the steady state and its radius is constant for as long as mass is being added at the source. Following the spill shut-off, the pool gradually shrinks in size as the liquid is depleted by evaporation.

A feature which is observed in many of the cases simulated using the present method is the separation of an annular region containing a small amount of LNG from the main pool just prior to reaching the steady state. Although no clear experimental evidence for the existence of such a wavelet was found, an argument substantiating the present result will be offered later in this section. Assuming for the moment that the outward propagating wavelet exists under idealized conditions, it is noted that the real surface conditions (i.e. waves) could be expected to disperse the LNG contained therein.

The two cases just described represent the two extremes in categorizing a spill. There must exist a degree of overlap, when for instance, a continuous spill is executed so quickly that in the limit it may be considered as instantaneous. In reality, that is how an instantaneous

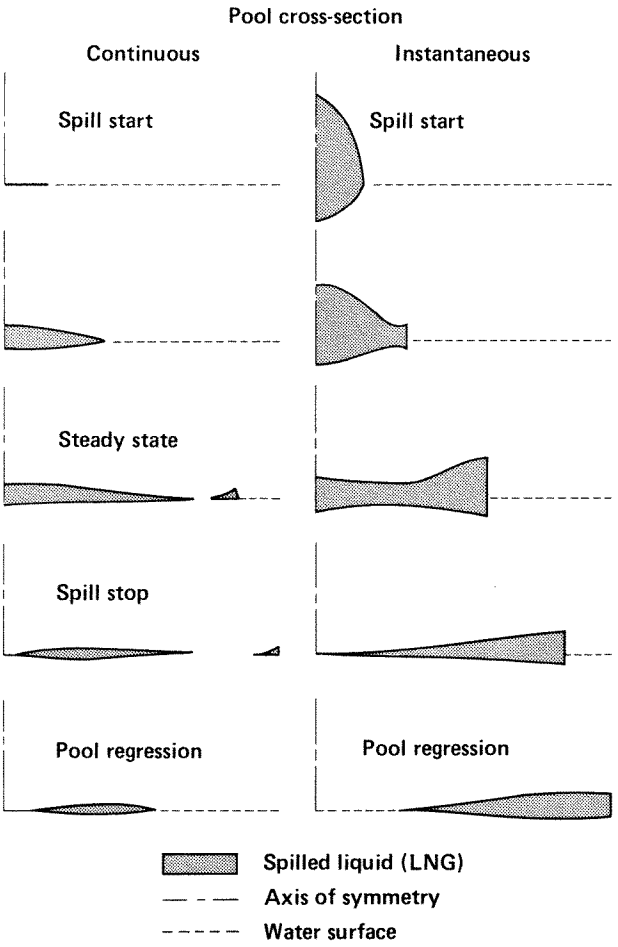


Figure 1. Schematic representation of the evolution of a continuous and instantaneous spill of LNG on water

release is accomplished. Raj[6] addressed the question of classifying spills but did not investigate the structural differences characterizing these spills. This will be attempted in the present section.

First, results are shown in Figure 2 for the location of the pool's leading edge as a function of time for an LNG spill of 0·0817 $m^3$. Presented on this graph are the computed results for the instantaneous and several continuous spills of that volume, as well as the available experimental results from Reference 10 for the instantaneous case (batch spill). It is interesting, that the experimental data show the best agreement with the simulated release one second in duration. This may not be surprising if it is noted that the experimental instantaneous spill was carried out by tipping a bucket of LNG onto a water surface. In view of this, the agreement between the experimental and computed results is considered to be quite satisfactory. Another important implication from Figure 2 is the observation that the instaneous limit is smoothly approached by decreasing the spill time (while keeping the total spill mass constant) in the numerical simulation. This is also seen for the case of a 250 $m^3$ spill (4 orders of magnitude greater) in Figure 3. (The appearance of multiple values of pool radius in the 100 second duration spill in Figure 3 will be addressed later.)

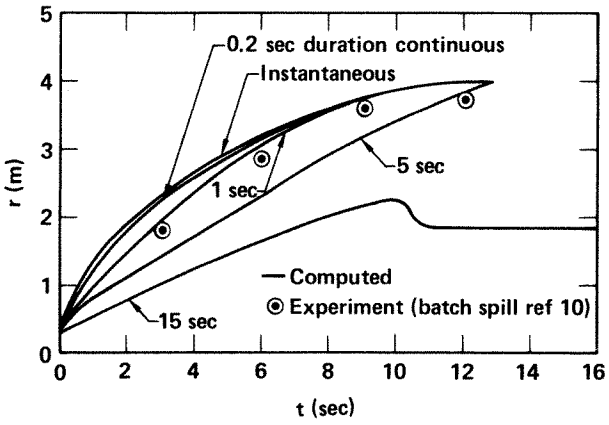


Figure 2. Comparison of the variation of the pool's outer radius for several continuous and an instantaneous spill of 0·0817 $m^3$ of LNG on water

Next, the results of numerical simulations, both for instantaneous and continuous spills in the range $0{\cdot}0817 \leq V \leq 25{,}000\ m^3$ are plotted in Figure 4 using Raj's[6] similarity variables

$$\xi = \frac{R_{MAX}}{V^{1/3}}; \qquad \tau_t = \frac{tv}{V^{1/3}} \tag{6}$$

The present results show good agreement with those obtained in Reference 6. They confirm the validity of the similarity variables $\xi$ and $\tau_t$ for continuous spills. In the case of instantaneous spills, the present results show greater spread and consequently, the cross-over time appears more aptly to be described by the band $10^{-3} < \tau_t < 5 \times 10^{-3}$ rather than a point as indicated in Reference 6.

It has been stated earlier that the instantaneously spilled pools were found to regress from the centre outward whereas the opposite was computed for the continuous spills which reached a steady state. It is seen in Figure 5 that a continuous spill which was terminated

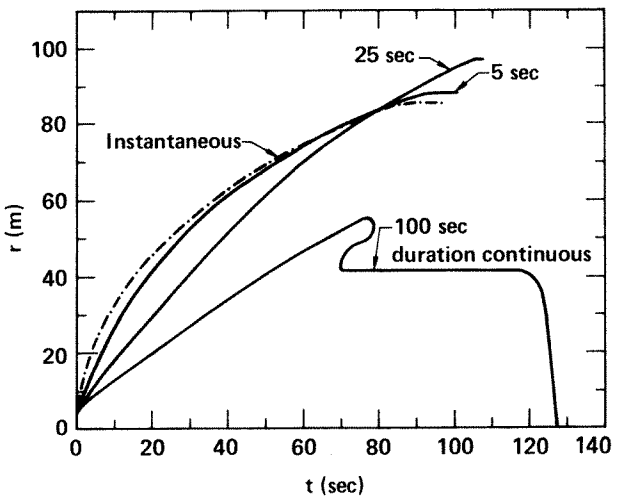


Figure 3. Comparison of the variation of the pool's outer radius for several continuous and an instantaneous spill of 250 $m^3$ of LNG on water

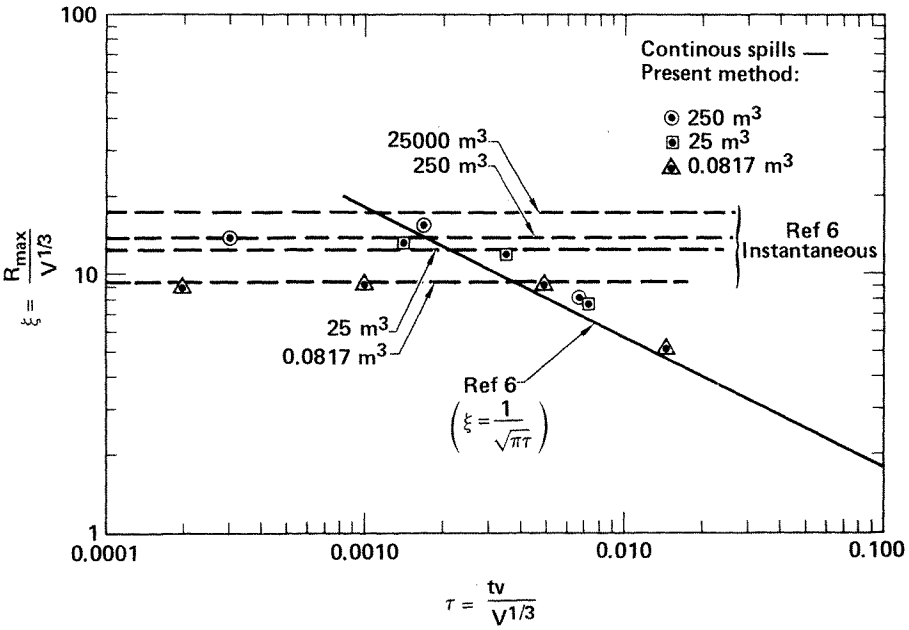


Figure 4. Maximum radius of spread as a function of spill time for instantaneous and continuous spills of LNG on water in terms of non-dimensional parameters ($0{\cdot}08 \leq V \leq 25{,}000\ m^3$)

before reaching steady state, exhibits the same centre-originating regression seen for instantaneous spills. Indeed, examination of Figure 5 reveals that this short duration release resembles an instantaneous spill. Such a similarity increases as the spill duration decreases as further evident in Figures 2 and 3.

It is now convenient to re-address the subject of the leading edge wavelet which according to the computed, continuous spill results, was found to separate from the main pool just prior to steady state. The wavelet is indicated in Figure 5 as the appendix-like projection causing the pool radius to be multi-valued. It is noted that the time needed for total evaporation of the LNG contained within the wavelet was sensitive to the radial step size used for the computation. Since the separating wavelet contained only an insignificant

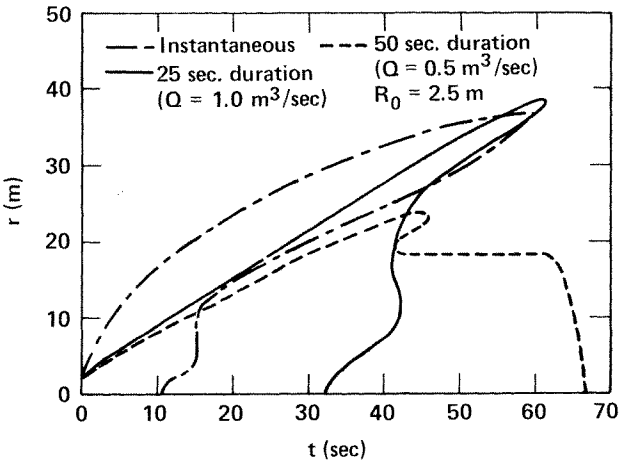


Figure 5. Pool envelope as a function of time for continuous and instantaneous spills of 25 $m^3$ of LNG on water

fraction of the total volume of LNG spilled, its quantitative aspects will not be discussed. However, the following qualitative argument is offered in support of the existence of the wavelet.

Since the spill takes place on water, the high-momentum fluid in the leading edge of the pool thickens (to form a shock), owing to water resistance to the partially submerged, spreading LNG. Behind the leading edge the pool thickness is smallest, as the fluid there is 'stretched' owing to the velocity gradient. In consequence of this 'stretching' and, simultaneously, due to evaporation, the leading edge wavelet separates from the main body of the pool (which subsequently reaches its maximum, steady state radius) and travels outwards until all the material evaporates. This is similar to the scenario describing the instantaneous spill, and, indeed, the results in Figure 5 support this interpretation.

## INSTANTANEOUS SPILLS

Good agreement was seen for continuous spills between the present results and simple algebraic formulation (i.e. Reference 6) for the maximum pool radius as well as for the time it takes to reach it. For the case of instantaneous spills such a comparision is not as favourable, as shown in Figure 6. The algebraic approach significantly underestimates the

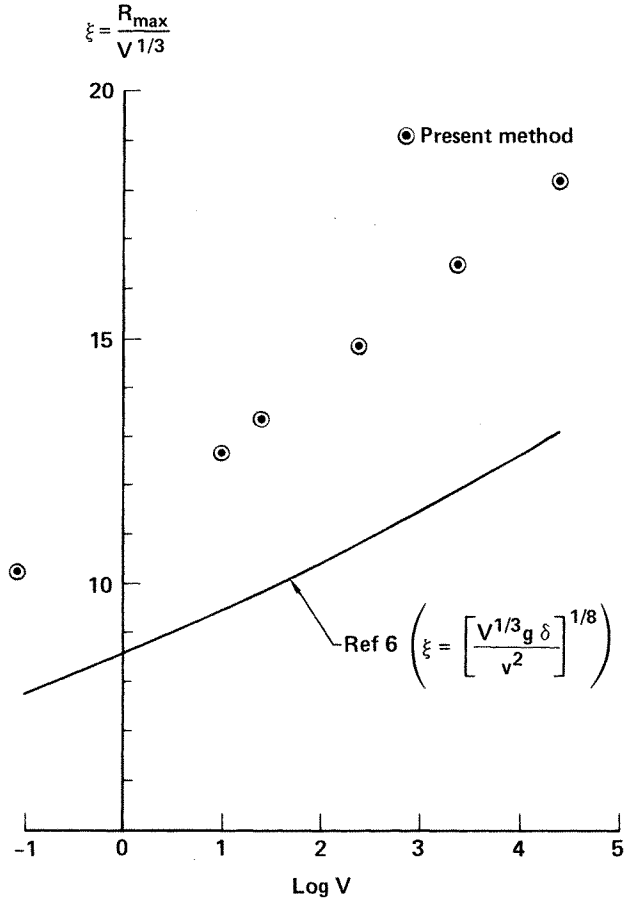


Figure 6. Nondimensional pool radius vs log $V$ for instantaneous spills of LNG on water within the range $0{\cdot}08 \leq V \leq 25{,}000\ m^3$

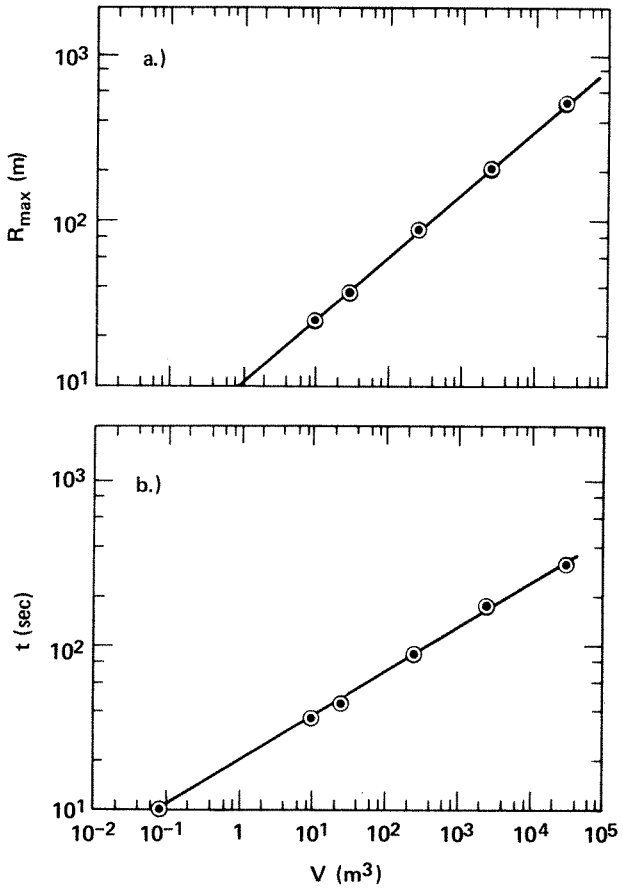


Figure 7. Steady state pool radius and time to steady state vs spill volume for instantaneous spills of LNG on water within the range $0{\cdot}08 \leq V \leq 25{,}000\ m^3$

pool radius. A similar order of magnitude relation for time to reach the maximum radius was even more in error.

A simple empirical relation could be derived for variation of maximum radius with volume spilled and for variation of time to reach the maximum radius with volume spilled by examining Figure 7. Over the six orders of magnitude of volume ranging from a laboratory-size spill of $0{\cdot}08\ m^3$ to a supertanker-size spill of $25{,}000\ m^3$, these relationships are linear on the log–log plot. In general, they may be written:

$$\log R_{MAX} = A \log V + \log B \tag{7}$$

$$\log T = C \log V + \log D \tag{8}$$

where the constants $A$, $B$, $C$, and $D$ are functions of the liquid spilled and of the spill surface. For the present case of LNG spills on water, using units of metres for length and seconds for time, and after determining the constants, equations (7) and (8) can be expressed:

$$R_{MAX} = 10{\cdot}0 V^{0{\cdot}386} \tag{9}$$

$$T = 19{\cdot}7 V^{0{\cdot}266} \tag{10}$$

## CONTINUOUS SPILLS

*Effect of the radius of the source*

The primary effect of increasing the radius of the source, while keeping the mass inflow rate, $Q$, constant was seen to be the decrease in the rate of spread of the pool. An indication of this is presented in Figure 8, where time needed to reach steady state is plotted as a function of source radius for the vaues of $Q$ of $1/m^3/s$ and $0{\cdot}233\ m^3/s$. This is readily explained by arguing that in order to keep $Q$ constant, the momentum imparted to the injected fluid increases as the source radius decreases. The pool radius, corresponding to steady state, did not vary with the source radius.

*Effect of the shear stress*

A commonly used expression for the effect of viscosity in the shallow water equations is the Chezy resistance expression.[11] The shear stress is taken as proportional to $u^2$ and inversely proportional to $h$. Adapting this functional relationship, the viscous term in equation (2) is written as

$$\frac{\tau}{\rho h} = \frac{C|u|u}{\rho h} \quad \text{where} \quad C \ll 1{\cdot}0 \tag{11}$$

This form allows reversal in the direction of action of the shear stress corresponding to reversal in the flow direction. Unfortunately, the proportionality constant, $C$, has to be

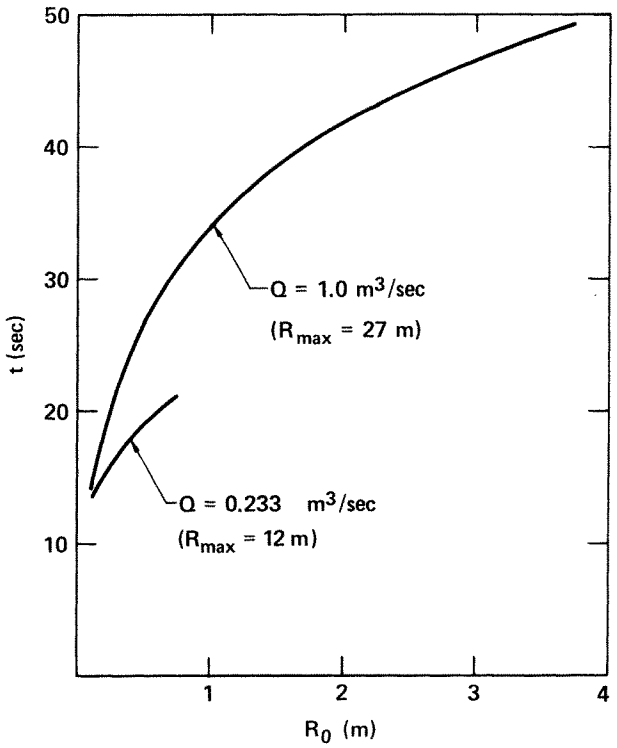


Figure 8. Time to steady state as a function of the source radius for two discharge rates of LNG on water

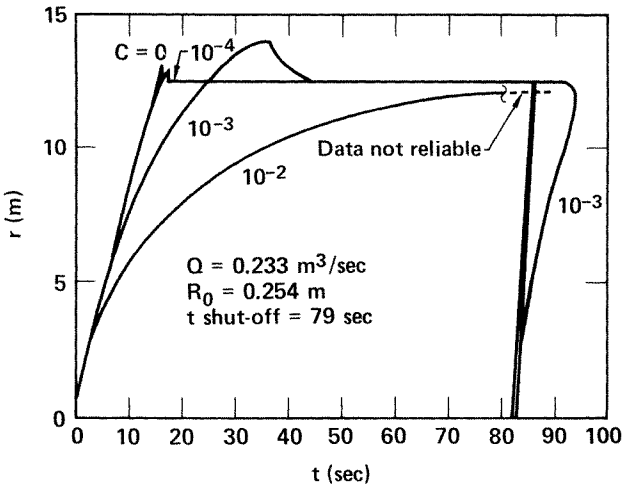


| | C = 0 | C = $10^{-4}$ | C = $10^{-3}$ | C = $10^{-2}$ |
|---|---|---|---|---|
| $R_{ss}$ (m) | 12.5 | 12.5 | 12.5 | Not reached |
| $T_{ss}$ (sec) | 16.9 | 19.1 | 44.5 | Not reached |
| LNG Present in the main pool ($m^3$) | 1.2 | 1.2 | 2.2 | 5.7 |
| LNG Present in the wave ($m^3$) | 1.1 | 0.8 | None | None |

Figure 9. Influence of the viscosity coefficient on the spreading of 18·4 $m^3$ continuous spill of LNG on water

empirically determined. Nevertheless, the above expression is very useful in studying the functional dependence of the solution on the shear stress. The results for a continuous spill of 18·4 $m^3$ over the duration of 79 s, computed for the values of the shear coefficient, $C$, ranging between 0 and 0·01 are presented in Figure 9. These results indicate a significant effect of the shear forces on the rate of spread of the liquefied fuel. The location of the leading edge, which for zero-shear was a linear function of time (except in the vicinity of the origin), assumes significantly non-linear variation with time as $C$ is increased. Correspondingly, the time needed to reach the steady state increases rapidly with the value of $C$. The steady state radius was observed to be invariant with the value of the shear coefficient, except in the case of the highest value used ($C = 0{\cdot}01$) for which the equilibrium is never reached. This case appears to be overdamped. The pool radius never reaches its maximum, steady-state values, although the spill duration is four times longer than that required to reach steady state with $C = 0$. An additional observation concerning the effect of shear could be made on the basis of integrating the volume of LNG present in the pool at steady state and in the annular wave that separated just before the steady state is reached. Thus, the increase in shear tends to eliminate the separated wave while increasing the volume of lNG present in the pool as the result of increased pool thickness. The former observation is easily understood, by recalling that the retarding effects are concentrated close to the leading edge. The latter effect is the result of the slower rate of spread of the pool. Since the time needed

to reach the steady state increases, more LNG accumulates within the pool, as more liquefied fuel is being added at the source than can evaporate.

Next, an attempt is made to determine a realistic value of the constant $C$ for the batch spill of 0·0817 m$^3$ of LNG, for which the experimental results have been reported in Reference 10. Using the arguments put forward in the discussion pertaining to Figure 2, the numerical simulation was carried out for an equivalent spill, one second in duration. The computed results, using $C = 5 \times 10^{-4}$ are seen (Figure 10) to be in very good agreement with the experimental data.[10] This particular value of $C$ has been chosen empirically, and can be expected to give good results only for this case. Clearly, a formulation of the viscous term in a manner avoiding the need for an empirical constant would be preferable. Such a formulation was given in Reference 2. Following Fannelop and Waldman[2] who use the drag relation for Rayleigh flow, the shear stress is written

$$\tau = \sqrt{\left(\frac{\rho\mu}{\pi}\right)} \frac{u}{\sqrt{t_R}} \tag{12}$$

Since the product $\rho\mu$ is over twenty times greater for water than it is for LNG, the water surface may be idealized as a rigid plane with the fluid (LNG) flowing over it. (A similar argument has been presented in Reference 2 for the cases of oil flowing over water to justify the derivation of an expression equivalent to equation (12).) Consequently, $\rho$ and $\mu$ are taken as density and viscosity of LNG, and $u$ is the local flow velocity. The parameter $t_R$ is a characteristic time and it will be defined here as an average time in motion expressed as

$$t_R = \frac{r_{LE}}{\bar{u}}; \qquad \bar{u} = \sum_i^N \frac{u_i}{N} \tag{13}$$

where $i$ is a summation index and $N$ is the number of grid points within the pool. Using the physical values of $\rho$ and $\mu$, equation (12) is re-written:

$$\frac{\tau}{\rho h} = 0{\cdot}29 \times 10^{-3} \frac{u}{h\sqrt{t_R}} \tag{14}$$

The results corresponding to the use of the drag law (equation (14)) are included in Figure 10. They are identical with the results obtained using equation (11) with $C = 5{\cdot}0 \times 10^{-4}$ to

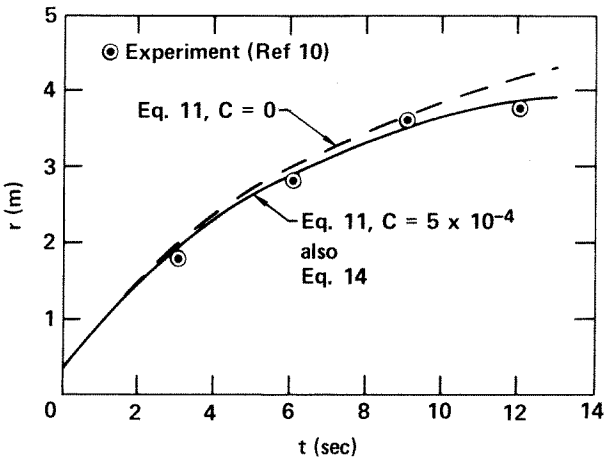


Figure 10. Comparison of two drag models with experimental data for the spill of 0·0817 m$^3$ of LNG. (Experimental data (Reference 10) for batch spill. Computed results for one second duration spill)

within the accuracy inherent in the grid spacing ($\Delta r \simeq 0{\cdot}06\ m$). It is therefore suggested that the two drag terms (equation, (11) and (14)) are largely equivalent, if $C$ in equation (11) is approximated as

$$C \simeq \sqrt{\left(\frac{\rho\mu}{\pi}\right)} \frac{1}{\sqrt{(r_{LE}u)}} \tag{15}$$

*Effect of loss of surface cohesivity*

As stated earlier, the surface tension plays an important role in pool spread only in the late stages of the evolution of the spill, that is when the LNG thickness in the pool approaches a minimum thickness necessary for cohesivity. As this stage is reached, experiments[10] show that the film of LNG covering the water surface breaks up into discrete droplets. There is a disagreement[10,12] concerning the numerical value of the minimum cohesive thickness of LNG and whether or not it depends on the size of the spill. Here it was chosen, for simplicity to follow Reference 10 where that thickness is given as 0·17 cm and is taken as invariant with other properties of the spill. It is further assumed that following the pool break-up, all the LNG within the area where $h < \frac{h_{min}}{2}$, exists in the form of droplets. These droplets are taken to be hemispherical in shape and of the constant size $r_D = h_{min} = 0{\cdot}17$ cm. Then, knowing the volume, $V$, of LNG in the incremental area under consideration and defining

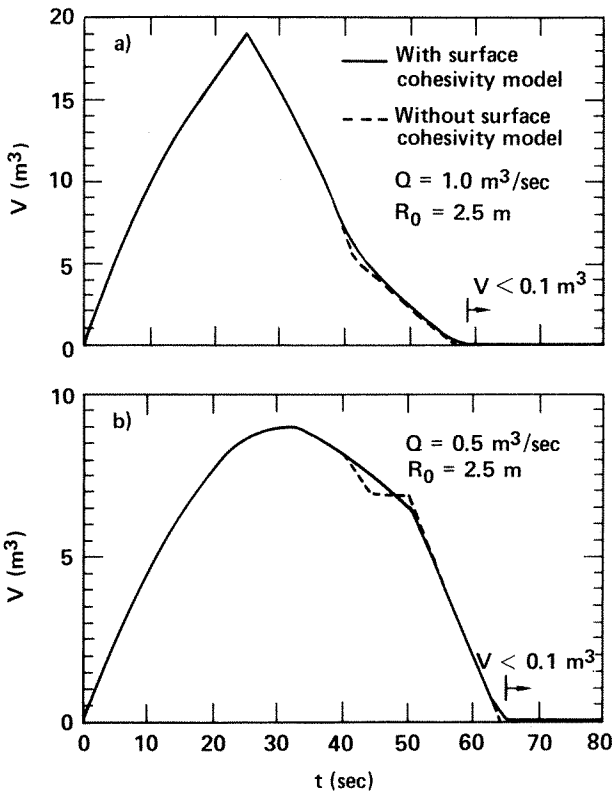


Figure 11. Volume of LNG in the pool as a function of time with and without the surface cohesivity model: (a) 25 m$^3$ discharged over 25 s, (b) 25 m$^3$ discharged over 50 s

the volume and the surface area of an individual, hemispherical droplet as

$$V_D = \tfrac{2}{3}\pi h_{min}^3 \tag{16}$$

$$A_D = 2\pi h_{min}^2 \tag{17}$$

the ratio of the total surface area of the droplet ensemble, $S$, to the geometric area, $A$, is

$$\frac{S}{A} = \frac{V}{V_D}\frac{A_D}{A} \tag{18}$$

This ratio is now regarded as the coefficient of the surface cohesivity. It is used to create a new, variable, locally valid regression rate

$$\tilde{v}(r, t) = v\frac{S}{A} \tag{19}$$

The results of including the surface cohesion model (equations (18) and (19)), in the formulation are shown in Figures 11 and 12. These results are for a 25 $m^3$ continuous spill from a source having a radius of 2·5 m. Two cases are shown: one, for a 25-second spill duration, and the other for a 50-second spill. These were computed under the assumption of zero friction at the surface. It is apparent from the volume vs. time plots (Figure 11), that the

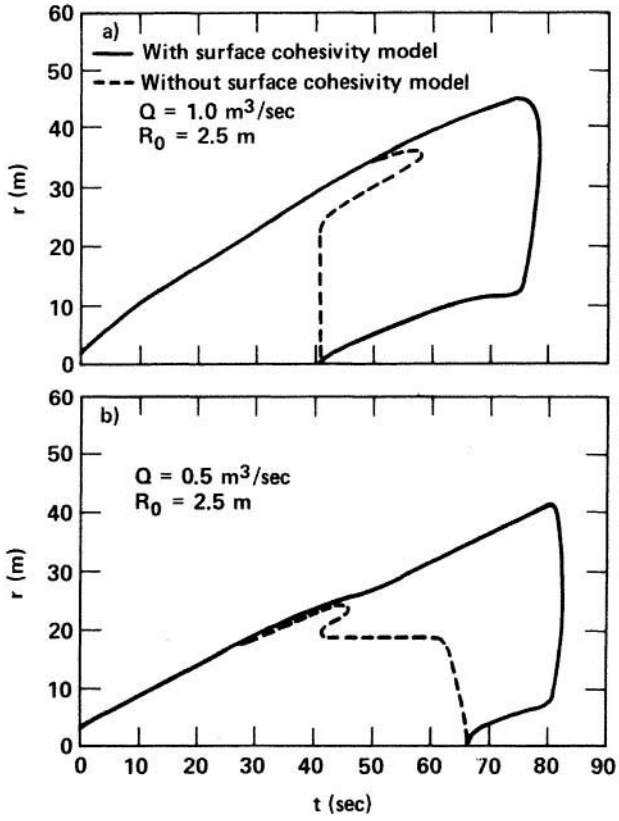


Figure 12. LNG pool envelope as a function of time with an without the surface cohesivity model: (a) 25 $m^3$ discharged over 25 s (b) 25 $m^3$ discharged over 50 s

surface tension adjustment had only a minor effect on the amount of LNG in the pool at any given time. It is seen though, that the model predicts a small amount of liquid present for up to 15 s beyond the time for total evaporation computed without accounting for loss of surface cohesion. This is much clearer in Figure 12, showing the surface covered by LNG as a function of time. A disquieting feature appearing in Figure 12 is the apparent disappearance of the constancy of size of the pool at steady state. It must be emphasized though, that the additional area is covered by discrete LNG droplets and that the main cohesive part of the pool maintains its steady state dimensions. This apparent difficulty is easily cleared up by allowing frictional forces to dissipate all motion in the areas where pool break-up has occurred. It was observed earlier that for slower rates of discharge the depletion due to evaporation proceeds from the centre outwards, with the reverse true for the faster spills. With the addition of the surface tension effect, this qualitative difference vanished, and both cases show depletion from the centre outwards. Likewise, presence of LNG on the surface past the time for total evaporation computed using the present model without the surface adjustment has been noted experimentally.[10] These facts point towards at least the qualitative correctness of the model.

## CONCLUSION

A simple, numerical model based on the shallow water equations has been applied for simulation of continuous and instantaneous spills of LNG onto the water surface. Advantages of the model over the algebraic order- of magnitude approach have been pointed out. The similarities and differences in the pool structure for continuous and instantaneous spills have been examined. The results confirmed that a continuous spill over a short duration gives rise to the pool structure characteristic of an instantaneous spill. The general quantitative results agreed well with those in Reference 6. For instantaneous spills the maximum pool radius and the time to reach the maximum pool radius were found to vary linearily with the spill volume on the logarithmic plot. For continuous spills, increasing the radius of the source was found to decrease the rate of pool spreading. Models were also examined for inclusion of the shear stress and for the evaporation term so as to account for pool break-up. The application of the latter model resulted in a significant increase in time needed for total evaporation.

### ACKNOWLEDGEMENTS

Work performed under the auspices of the U.S. Department of Energy by the Lawrence Livermore National Laboratory under contract number W-7405-ENG-48.

## REFERENCES


1. J. Brandeis and E. J. Kansa, 'Numerical simulation of liquid fuel spills: I. Instantaneous release into confined area, (1981).
2. T. K. Fannelop, 'Dynamics of oil slicks', *AIAA Journal*, **10,** (4), 506–510 (1972).
3. W. G. May and P. V. K. Perumal, 'The spreading and evaporation of LNG on water'. 74-WA/PID-15, presented at the *Winter Annual Metting of ASME*, N.Y. 17–22 November 1974.
4. P. K. P. Raj and A. S. Kalelkar, 'Fire hazard presented by a spreading, burning pool of liquefied natural gas on water' presented at *Combustion Institute (USA) Western Section Meeting* (1973).
5. R. P. Koopman *et al.*, 'Burro series data report LLNL/NWC, spill tests', *UCID-19075*, (1980).
6. P. K. P. Raj, 'A criterion for classifying accidental liquid spills into instantaneous and continuous types', *Combustion Science and Technology*, **19,** 251–254 (1979).
7. J. A. Fay, 'The spread of oil slicks on a calm sea', in D. P. Hoult (ed.) *Oil and Sea*, Plenum Press, New York, 1969.
8. G. Opschoor, 'The spreading and evaporation of LNG—and burning LNG—spills on water', *Journal of Hazardous Materials*, **3,** 249–266 (1980).
9. G. A. Dainis and R. C. Reid, 'The boiling and spreading of liquified natural gas on water', Gas Research Institute, *GRI 80/0012*, (1980).
10. G. J. Boyle and A. Kneebone, 'Laboratory investigations into the characteristics of LNG spills on water', Shell Research Limited, Charter, England, *Report* 6*Z*32, (1973).
11. R. F. Dressler, 'Hydraulic resistance effect upon the dam-break function', *J. res. Nat. Bur. Stand.*, **49,** 217–225 (1952).
12. G. F. Feldbauer *et al.*, 'Spills of LNG on water', Esso Research and Engineering Company, *Report EE* 61 *E*-72, (1973).